

## Invited

## A Statistical Analysis of Microlithography

Henry I. Smith

Massachusetts Institute of Technology

Cambridge, Massachusetts, 02139, USA

Photo, x-ray, electron-beam, and ion lithographies are analyzed from a statistical point of view in order to relate linewidth control to the contrast of the exposure technique, exposure uniformity, and the resist contrast and sensitivity. We show that the use of UV projection lithography for  $0.5\ \mu\text{m}$  linewidths will require very precise control of exposure uniformity as well as high-contrast resist. We also compare the maximum pixel-transfer rates of the various lithographies.

Many decades ago the problem of noise in photographic imaging and CRT displays was analyzed, and criteria established for the number of photons or electrons required per picture element, or "pixel". Although microlithography bears a close relationship to classical imaging, the problem of noise and criteria for the number of particles required per pixel are quite different in the two cases. For example, there are no grey tones in microlithography: a pixel should be either fully exposed or fully unexposed. Also, microlithography, at least as applied to integrated electronics, demands a much lower probability of error than does most imaging. Lastly, linewidth control is a criterion of major importance in microlithography. In this paper we review and expand an earlier analysis<sup>1)</sup> of the consequences of the stochastic nature of the exposure process, and on this basis compare the several lithographic techniques. Earlier, Spiller and Feder discussed the statistics of x-ray exposure, and derived equations relating maximum permissible resist sensitivity to pattern resolution and mask contrast<sup>2)</sup>.

We consider the exposure of a test pattern, a one-dimensional grating of spatial-period  $p$ . The pattern is conceptually subdivided into discrete square "pixels" of

edge dimension  $\varepsilon$ . In this analysis we choose  $\varepsilon = p/20$ . Linewidth,  $w$ , depends on exposure time and resist properties, and can vary within the range  $\varepsilon$  to  $p$ . Usually, one tries to have  $w \sim p/2$ . We compare lithographic techniques primarily by considering linewidth control,  $\Delta w$ . We include in  $\Delta w$  both the uncertainty in the average linewidth and ripple along the edge of a line.

For photon-based lithographies (i.e., photolithography and x-ray lithography) we use the cubic pixel model<sup>1)</sup> and restrict our attention to a single layer of cubic pixels within the resist (i.e., a layer of thickness  $\varepsilon$ ). For a homogeneous resist film this layer should be located at the resist-substrate interface where the flux of photons is minimum. For tri-level resists, resist systems with thin contrast-enhancement layers, or inorganic resists based on silver photodoping, this layer should be identified with the uppermost level. The present analysis can be generalized to any number of layers of pixels.

For electron and ion lithographies we use a model in which the pixels are parallelepipeds with square cross sections that extend through the full thickness of the resist film. When an electron enters a resist film it undergoes

scattering which quickly increases the spatial extent of the energy dissipation. For our purposes it will be adequate to use the model of T.H.P. Chang<sup>3,4)</sup> which describes the energy dissipation per unit volume,  $f(r)$ , with a double Gaussian expression

$$f(r) = k \{ \exp(-r^2/\beta_f^2) + \eta_E \exp(-r^2/\beta_b^2) \}, \quad (1)$$

where  $k$  is a proportionality constant,  $r$  is the radial distance from the beam axis,  $\beta_f$  is the Gaussian parameter for the forward scattering,  $\beta_b$  is the Gaussian parameter for the backscattering (much larger than  $\beta_f$ ), and  $\eta_E$  is the ratio of the volume integrated exposure by the backscattered electrons to that by the forward scattered electrons. The parameter  $\beta_f$  depends on film thickness and the spreading due to forward scattering, and can include the finite initial width of the beam.<sup>4)</sup> We will take

$$\epsilon = \beta_f. \quad (2)$$

For ion exposure we assume that ions pass completely through a resist film, exposing a right-circular cylinder about 10 nm in diameter. The mean distance, "a", between the axes of such exposure cylinders determines the mean number,  $\bar{N}$ , of ions incident per pixel area:

$$\bar{N} = 1.15\epsilon^2/a^2 \quad (3)$$

Consider now the exposure, for a fixed length of time, of the periodic grating test pattern in a single layer of pixels (either cubes or parallelepipeds). Let  $\bar{N}(x)$  represent either the mean number of photons absorbed in a cubic pixel volume, or the mean number of charged particles incident per pixel area, as a function of distance,  $x$ , perpendicular to the grating lines. We assume that any of the lithographic techniques will produce a  $\bar{N}(x)$  distribution that can be closely approximated by a region, one or more pixels wide, at  $\bar{N}_{\max}$ , a region of linearly decreasing count that is  $m$  pixels wide, a region of minimum count,  $\bar{N}_{\min}$ , that is one or more pixels wide, and a region of increasing count that is  $m$  pixels wide. The widths of the  $\bar{N}_{\max}$  and  $\bar{N}_{\min}$  regions need not be equal. When a lithographic technique is operated near the limit of its resolution, the function  $\bar{N}(x)$  should be approximately sinusoidal on a background. We approximate a sinusoi-

dal distribution with a piecewise-linear distribution<sup>1)</sup> in which  $m = 6$ . In all other cases  $m$  will be less than 6. The contrast function is given by

$$K = \Delta N / 2\bar{N}_m, \quad (4)$$

where  $\bar{N}_m$  is midway between  $\bar{N}_{\max}$  and  $\bar{N}_{\min}$ , and  $\Delta N = \bar{N}_{\max} - \bar{N}_{\min}$ .

If we now consider the actual number,  $N(x)$ , of photons absorbed per pixel, or charged particles incident per pixel area, during a fixed period of time, there will be deviations from the mean distribution as a result of statistical fluctuations. We assume that the arrivals of photons or charged particles are random events. Thus, the RMS deviation from  $\bar{N}$ ,  $\sigma$ , is given by

$$\sigma = \sqrt{\bar{N}(x)} \quad (5)$$

In Fig. 1,  $\bar{N}(x)$  is plotted along with functions corresponding to  $n$  standard deviations above and below  $\bar{N}(x)$ . Also indicated in Fig. 1 is a

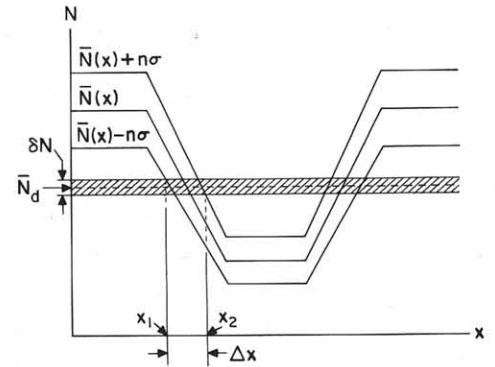


Figure 1: A plot depicting  $\bar{N}(x)$  and functions  $n$  standard deviations above and below  $\bar{N}(x)$ . The cross-hatched region,  $\delta N$ , centered on  $\bar{N}_d$ , is the development-uncertainty band. Pixels with  $N(x)$  above this band are fully developable, those with  $N(x)$  below are undevelopable. Development is uncertain for those pixels for which  $N(x)$  falls within the band.

band of values of  $N$ , centered on  $\bar{N}_d$  and designated as  $\delta N$ , which we call the development-uncertainty band. Pixels for which  $N(x)$  is above this band are fully developable. Pixels for which  $N(x)$  is below this band will be undeveloped. For pixels in which  $N(x)$  falls within the band it is uncertain whether or not they develop. The width of the development-

uncertainty band is a measure of the resist contrast (i.e., small  $\delta N$  corresponds to high contrast) and any variations in the exposure process, such as variation in intensity over the field-of-view, variation from one exposure to the next, or variation in resist thickness or response. (This expands the definition of  $\delta N$  in Ref. 1.)

Also illustrated in Fig. 1 is  $\Delta x$ , the uncertainty in the position of the line edge. This  $\Delta x$  is clearly dependent on the slope of  $\bar{N}(x)$  as well as on the width of  $\delta N$ .

A constraint which must be imposed is that  $\delta N$  be "n" standard deviations below  $\bar{N}_{\max}$ . The value of n is a matter of choice; it is related through the Poisson distribution to the probability that a pixel which is supposed to be developed remains undeveloped as a result of statistical fluctuations. If we assume  $\delta N$  is centered on  $\bar{N}_m$  this condition can be expressed

$$\bar{N}_{\max} - n (\bar{N}_{\max})^{1/2} > \bar{N}_m + \delta N/2 \quad (6)$$

or

$$\bar{N}_m > \frac{n^2 (1+K)}{K^2 (1-\delta N/\Delta N)^2} \quad (7)$$

Taking  $K = 1$  (the maximum possible value) and  $\delta N/\Delta N = 0$  (i.e., infinite resist contrast and perfect exposure control) we get

$$\bar{N}_m > 2 n^2 \quad (8)$$

This is the absolute minimum value for  $\bar{N}_m$ , which obtains even if  $m = 0$ . We will see below that  $\bar{N}_m$  is usually much larger than this.

The uncertainty in line edge position is given by<sup>1)</sup>:

$$(\Delta x/\epsilon) = (m/2K) [(\delta N/\bar{N}_m) + 2n/\sqrt{\bar{N}_m}] \quad (9)$$

The first term in the brackets reflects the error in line-edge position due to finite resist contrast and variations in the exposure process, since these are included in  $\delta N$ . The second term reflects the error in line-edge position due to fluctuations. Note that as resist sensitivity is increased (i.e.,  $\bar{N}_m$  is reduced) this second term increases.

#### Limits of Optical Projection Lithography

Let us consider what light eq. (9) can shed on the question of whether optical projection can be used in production for 0.5  $\mu m$  minimum

linewidths. At 0.5  $\mu m$  linewidth, an optical system is operated near its limit, that is,  $K = 0.5$  and  $m = 6$ . Letting  $(\Delta x/\epsilon) = 1$ , and  $n = 3$ , equation (9) gives

$$1 = 6 [(\delta N/\bar{N}_m) + (6/\sqrt{\bar{N}_m})] \quad (10)$$

For a resist with a sensitivity of 100 mJ/cm<sup>2</sup>,  $\bar{N}_m \sim 4 \times 10^5$  and equation (10) reduces to the requirement

$$\delta N/\bar{N}_m < 0.16. \quad (11)$$

It will likely be extremely difficult to meet this condition in production. For example, a variation in illumination of  $\pm 5\%$  over the field of view is very hard to achieve. Thus, this contributes 0.1 to  $\delta N/\bar{N}_m$ . Variation of resist sensitivity from batch to batch and from place to place on a wafer due to thickness variation and other factors may contribute perhaps 0.03. This leaves us with 0.03 for the intrinsic "contrast" of the resist. This is an extremely difficult requirement. PMMA is estimated to have an intrinsic  $\delta N/\bar{N}_m$  of about 0.1. Clearly, precise control of illumination uniformity and the use of very high contrast resist systems will be required to achieve  $\Delta x = \epsilon$ , that is, linewidth control of 20% ( $\Delta W = 2\epsilon$ ).

#### Throughput Comparisons

The statistical analysis of lithography, as summarized in Eq. (9), also enables one to compare the maximum throughputs of the various lithography techniques. We believe that the measure of throughput should not be "wafers per hour" but rather the equivalent "pixel-transfer-rate", R. With such a metric the various lithography techniques can be compared on the same footing. Needless to say, time spent in sample handling, movement or alignment is not included in R.

Allowing for the possibility that resists of extremely high contrast may be available in the future, and assuming no variation in exposure, we let  $\delta N/\bar{N}_m \sim 0$  in Eq. (9) (this minimizes  $\bar{N}_m$  and hence maximizes R). Setting  $\Delta x = \epsilon$ , (i.e.,  $\Delta w = 2\epsilon$ ), we obtain a simple expression for the statistically dictated minimum number of absorbed photons required per pixel, or incident charged particles required per pixel area:

$$N_m = n^2 m^2 / K^2. \quad (12)$$

(In the event that  $N_m$  calculated from Eq. (12) is less than  $N_m$  calculated from Eq. (7) or (3) the larger value should be used.) Expressions for R and resist sensitivity, S, for the various lithographies were derived in Ref. 1. Correcting these by replacing  $N_m$  in them with  $N_{max}$ , revised results are given in Table 1 for the case of 0.5  $\mu$ m linewidths.

Clearly, there is a significant pixel-transfer-rate advantage to UV projection lithography. Beyond UV, synchrotron-based x-ray lithography provides the highest pixel-transfer rate, with plasma-based x-ray and masked-ion-beam the next choices. Even a conventional Al<sub>K</sub> x-ray source operated at 1 KW provides an R well in excess of R for scanning e-beam or ion beam. The disparity between x-ray and e-beam becomes even more marked at linewidths below 0.5  $\mu$ m.

#### References

- 1) H. I. Smith, J. Vac. Sci. Technol. B, B4, 148 (1986).
- 2) E. Spiller and R. Feder, "X-ray Lithography", Chap. 3 of X-ray Optics, Vol. 22 Topics in Applied Physics, Springer-Verlag, Berlin, 1977, Ed. H.J. Queisser.
- 3) T.H.P. Chang, J. Vac. Sci. Technol. 12, 1271 (1975).
- 4) R.J. Hawryluk, J. Vac. Sci. Technol. 19, 1 (1981). (a review)
- 5) D. Nagel, "Plasma Sources for X-ray Lithography". VLSI Electronics: Microstructure Science, Vol. 8, Ed. N. G. Einspruch, Academic Press, New York, 1984.
- 6) I. Okada, Y. Saitoh, S. Itabashi and H. Yoshihara, J. Vac. Sci. Technol. B, B4, 243 (1986).

This work was sponsored by the Joint Services Electronics Program.

Table 1

Comparison of maximum pixel transfer rates, R, for the various lithographies at linewidth  $W = 0.5 \mu$ m and  $\Delta W = 0.1 \mu$ m, assuming infinite resist contrast and perfect exposure control (i.e.,  $\delta N/N_m = 0$ ). S is minimum permissible resist dose.

Lithography Technique	Footnote	$N_m$	S	R (Hz)
Optical projection	(a)	1300	$0.5 \text{ mJ/cm}^2$	$8 \times 10^{13}$ to $8 \times 10^{16}$
X-ray (conventional)	(b)	24	$42 \text{ mJ/cm}^2$	$5.3 \times 10^8$
X-ray (plasma)	(c)	24	$27 \text{ mJ/cm}^2$	$1 \times 10^{10}$ to $6 \times 10^{11}$
X-ray (synchrotron)	(d)	24	$27 \text{ mJ/cm}^2$	$1.4 \times 10^{12}$
Scanning e-beam	(e)	900	$6 \mu\text{C/cm}^2$	$1.3 \times 10^7$
Scanning ion beam	(f)	29	$0.18 \mu\text{C/cm}^2$	$2.3 \times 10^7$
Masked ion beam	(g)	29	$0.18 \mu\text{C/cm}^2$	$2.1 \times 10^{11}$

#### Footnotes to Table 1

- Assumes:  $\lambda = 310 \text{ nm}$ ,  $\epsilon = 50 \text{ nm}$ ,  $n = 3$ ,  $m = 6$ ,  $K = 0.5$ , incident power of 1 to  $10^3 \text{ W}$ , and 10% absorption in a pixel.
- Assumes:  $\lambda = 0.834 \text{ nm}$ ,  $\epsilon = 50 \text{ nm}$ ,  $n = 3$ ,  $m = 1$ ,  $K = 0.82$ , input power to source of  $10^3 \text{ W}$ , and 1% absorption in a pixel.
- Assumes:  $\lambda = 1.24 \text{ nm}$ ,  $\epsilon = 50 \text{ nm}$ ,  $n = 3$ ,  $m = 1$ , and  $K = 0.82$  and 1% absorption. The first R value is for 20J laser pulses at 1 Hz onto a target with 25% conversion into useful x-rays emitted into  $2\pi$  steradians<sup>5)</sup>. The second R value is for a pulsed-plasma x-ray source with 600 W output into  $4\pi$  steradians.<sup>6)</sup>
- Assumes:  $\lambda = 1.24 \text{ nm}$ ,  $\epsilon = 50 \text{ nm}$ ,  $n = 3$ ,  $m = 1$ ,  $K = 0.82$ , incident power of 1W, and 1% absorption.
- Assumes: brightness of  $10^6 \text{ A/cm}^2 \text{ Sr}$ ,  $\alpha = 5 \times 10^{-3}$ ,  $\beta_f = 60 \text{ nm}^4$ ,  $K = 0.5$ ,  $\epsilon = 60 \text{ nm}$ , and  $m = 5$ .
- Assumes: brightness of  $10^6 \text{ A/cm}^2 \text{ Sr}$ ,  $\alpha = 10^{-3}$ ,  $m = 1$ ,  $K = 1$ ,  $\epsilon = 50 \text{ nm}$ , and  $a = 10 \text{ nm}$ .
- Assumes:  $m = 1$ ,  $K = 1$ ,  $a = 10 \text{ nm}$ ,  $\epsilon = 50 \text{ nm}$ ,  $1 \mu\text{A/cm}^2$  incident ion current density, and a  $1 \text{ cm}^2$  mask area.